Correlation of four-dimensional ultrasound strain analysis with computed tomography angiography wall stress simulations in abdominal aortic aneurysms

Wojciech Derwich, MD, MHBA,[a] Manuel Schönborn, MEng,[b] Christopher Blase, RNDr,[b] Andreas Wittek, Dr-Ing,[b] Kyriakos Oikonomou, MD, PhD,[a] Dittmar Böckler, MD, PhD, MHBA,[c] *and* Philipp Erhart, MD, PhD, MHBA,[c] *Frankfurt/Main, Germany; and Heidelberg, Germany*

ABSTRACT

Objective: Biomechanical modeling of infrarenal aortic aneurysms seeks to predict ruptures in advance, thereby reducing aneurysm-related deaths. As individual methods focusing on strain and stress analysis lack adequate discretization power, this study aims to explore multifactorial characterization for progressive aneurysmal degeneration. The study's objective is to compare stress- and strain-related parameters in infrarenal aortic aneurysms.

Methods: Twenty-two patients with abdominal aortic aneurysms (AAAs) (mean maximum diameter, 53.2 ± 7.2 mm) were included in the exploratory study, examined by computed tomography angiography (CTA) and three-dimensional real-time speckle tracking ultrasound (4D-US). The conformity of aneurysm anatomy in 4D-US and CTA was determined with the mean point-to-point distance (MPPD). CTA was employed for each AAA to characterize stress-related indices using the semi-automated A4-clinics RE software. Five segmentations from one 4D-US examination were fused into one averaged model for strain analysis using MATLAB and the Abaqus solver.

Results: The mean MPPD between the adjacent points of the 4D-US and CTA-derived geometry was 1.8 ± 0.4 mm. The interclass correlation coefficients for all raters and all measurements for the maximum AAA diameter in 2D, 4D ultrasound, and CTA indicate moderate to good reliability (interclass correlation coefficient$_1$ 0.69 with 95% confidence interval [CI], 0.49-0.84; $P < .001$). The peak wall stress (PWS) correlates fairly with the maximum AAA diameter in 2D-US ($r = 0.54$; $P < .01$) and 4D-US ($r = 0.53$; $P < .05$) and moderately strongly with the maximum exterior AAA diameter ($r = 0.63$; $P < .01$). The peak wall rupture risk index shows a strong correlation with the PWS ($\rho > 0.9$; $P < .001$) and is influenced by anatomical parameters with equal strength. Isolated observation of the intraluminal thrombus does not provide significant information in the determination of PWS. The maximum AAA diameter in 2D-US shows a fair negative correlation with the mean circumferential, longitudinal and in-plane shear strain ($\rho = -0.46$; $r = -0.45$; $\rho = -0.47$; $P < .05$ for all). The circumferential strain ratio as an indicator of wall motion heterogeneity increases with the aneurysm diameter ($r = 0.47$; $P < .05$). The direct comparison of wall strain and wall stress indices shows no quantitative correlation.

Conclusions: The strain and stress analyses provide independent biomechanical information of AAAs. At the current stage of development, the two methods are considered complementary and may optimize a more patient-specific rupture risk prediction in the future. (JVS—Vascular Science 2024;5:100199.)

Keywords: 4D-US; AAA; All strain; FEA; Ultrasound strain imaging; Wall stress

Modern medicine requires patient-personalized therapy planning. However, methods to predict individual rupture risk in abdominal aortic aneurysms (AAAs) are not fully validated. Because epidemiological data with the maximum aneurysm diameter offers uncertain statements, biomechanical analyses emerge to predict patient-specific rupture risk.[1] Stress and strain analysis has been proposed to gain further insight into disease progress and rupture risk beyond the diameter criterion. The concept of mechanical strength analysis postulates that rupture occurs at the site of the highest stress when the cumulative stress exceeds the local strength of the aneurysm wall.[1] In most cases, aortic wall stress is estimated using finite element analysis (FEA), which is

From the Vascular and Endovascular Surgery, Department of Cardiac and Vascular Surgery, University Hospital Frankfurt Goethe University, Frankfurt/Main[a]; the Personalized Biomedical Engineering Lab, Frankfurt University of Applied Sciences, Frankfurt/Main[b]; and the Department of Vascular and Endovascular Surgery, Heidelberg University Hospital, Heidelberg.[c]

Correspondence: Wojciech Derwich, MD, MHBA, Vascular and Endovascular Surgery, Department of Cardiac and Vascular Surgery, University Hospital Frankfurt Goethe University, Theodor-Stern-Kai 7, Frankfurt/Main 60590, Germany (e-mail: wojderwich@hotmail.com).

The editors and reviewers of this article have no relevant financial relationships to disclose per the Journal policy that requires reviewers to decline review of any manuscript for which they may have a conflict of interest.

2666-3503

https://doi.org/10.1016/j.jvssci.2024.100199

highly dependent on geometry, material properties, and underlying boundary conditions—all of which are highly patient-specific.[2] On the other hand, in vitro bulge-inflation tests on tissue specimens of human ascending thoracic aortic aneurysm wall tissue showed that rupture does not necessarily happen in the regions with the maximum stress, but rather in the wall areas with pathological strain patterns and localized thinning of the wall.[3]

The theory of stress analysis in simulations of aneurysm rupture has over 20 years of experience. Cohort-related analyses indicate biomechanical differences among asymptomatic, symptomatic, and ruptured abdominal aortic aneurysms using peak wall stress (PWS), peak wall rupture risk index (PWRI), and rupture risk equivalent diameter (RRED).[4] However, these parameters alone provide limited rupture prediction of aneurysm for individual patients.[5] Previous stress-based analyses were derived from AAA geometry in computed tomography angiography (CTA), considering patient-specific clinical information and population-averaged homogeneous biomechanical aortic wall properties. After improving the spatial resolution of sonographic diagnostics, four-dimensional ultrasound (4D-US) finds new applications in biomechanical modeling of AAAs. 4D-US allows not only adequate dynamic visualization of aneurysm geometry but also the detection of local AAA wall strains, complementing the limitations of FEA to optimize patient-specific rupture risk in AAAs.[6-8]

In contrast to the calculated parameters of stress analysis, strain analysis provides information about the actual measured deformation of the aneurysm wall and can use all advantages of a noninvasive 4D-US. Strain is a relative length change of an examined segment in a circumferential or longitudinal direction. Shear strain describes a relative shape change. High spatial and temporal resolution of the strain analysis allows discrimination between healthy, atherosclerotic and aneurysmal aortas based on strain amplitude and heterogeneity.[9] Despite the low strain amplitudes in AAA, the method's capacity enables the characterization of local wall deformation with kinematic distinction between the infrarenal neck and AAA sac,[7] as well as a detection of changes in the AAA strain pattern within longitudinal observations.[10] Moreover, the high spatial and temporal resolution of the detected wall deformation opens new perspectives for the biomechanical characterization of the aneurysm wall, determining elastic properties such as compliance or distensibility.[11-13]

The stress (FEA analysis) and strain analyses (4D-US) have been independently used to investigate AAA rupture risk predictors. Because the current methods of stress and strain analysis do not yet have sufficient discriminatory power between asymptomatic and rupture-prone AAAs, further synergies between the methods are sought with the aim of considering the nature of aneurysm rupture multifactorially and thus optimizing rupture prediction. However, the interactions between stress- and strain-related indices from two imaging methods have not been described for aneurysms so far. We hypothesize that 4D-US-derived wall strain parameters may have a highly significant correlation with anatomic features and CTA-based indices of wall stress in AAAs.

ARTICLE HIGHLIGHTS

- **Type of research:** Modeling study
- **Key Findings:** Abdominal aortic aneurysms (AAAs) in 22 patients were comprehensively characterized through stress and strain analyses utilizing computed tomography angiography and four-dimensional ultrasound, respectively. For each aneurysm, detailed assessments included morphological features, wall stress indices, and wall motion indices.
- **Take Home Message:** The wall stress indices exhibit a strong correlation with morphological features, whereas strain-related parameters independently describe the properties of the aneurysm wall, regardless of the wall stress indices and AAA anatomy. Stress and strain analysis complementarily characterize AAA properties and may enhance the identification of at-risk patients.

METHODS

Study design. The study comprises 22 consecutive patients (20 males and 2 females) (Table I) with asymptomatic AAA and typical comorbidities (Table II) examined by 4D-US and CTA (Fig 1). The inclusion criterion was the availability and sufficient quality of 4D-US in the presence of CTA with a slice thickness <2 mm in the arterial phase. Written informed consent from all patients for the use of data, as well as approval from the local ethics committee (no. 275/17 and S-462/2017), was obtained. CTA scans enable: (1) comparison of AAA geometry in CTA and 4D-US; (2) semi-automatic stress analysis using FEA (A4clinicRE software, VASCOPS GmbH). 4D-US strain analysis was performed based on the averaged models from five segmentation runs according to the methodology of Wittek and Hegner et al.[14,15] Segmentation and analysis of CTA, as well as registration with segmentation of 4D-US imaging, were performed by three independent investigators. We have not proven the interobserver variability of single examinations,[16] reliability of the segmentation process, and value of the averaged models for 4D-US,[14,15,17] as well as the reliability of the segmentation of the geometry and stress analysis for CTA[18] once again, because these processes have already been published and classified as reliable. However, we registered the conformity of AAA geometry in the 4D-US and in the gold standard CTA as

Table I. Patient characteristics with clinical parameters (n = 22)

	Mean ± SD	95% CI	Median (min; max)	IQR
Age, years	70.8 ± 6.6	67.9-73.7	71.5 (55.0-82.0)	69.0-74.5
Height, m	1.8 ± 0.1	1.7-1.8	1.8 (1.6-2.0)	1.7-1.8
Weight, kg	89.9 ± 15.3	82.9-96.8	87.0 (56.0-115.0)	80.0-100.0
BMI, kg/m^2	28.8 ± 4.2	26.9-30.7	28.1 (18.9-37.2)	26.8-31.6
Systolic systemic blood pressure, mmHg	140.2 ± 21.5	130.7-149.8	140.0 (110.0-180.0)	130.0-143.8
Diastolic systemic blood pressure, mmHg	80.7 ± 8.6	76.9-84.5	80.0 (60.0-100.0)	80.0-85.0

BMI, Body mass index; *CI*, confidence interval; *IQR*, interquartile range; *SD*, standard deviation.

Table II. Comorbidities of the study patients

Comorbidity	No.	%
Nicotine consumption (past and present)	11	50.0
Diabetes mellitus	2	9.1
Obesity (BMI >30 kg/m^2)	9	40.9
Arterial hypertension	18	81.8
Hyperlipidemia	14	63.6
Peripheral arterial occlusive disease	5	22.7
History of an ischemic stroke	5	22.7
Coronary heart disease	9	40.9
Chronic kidney disease	3	13.6
Chronic obstructive pulmonary disease	4	18.2
Aneurysms in other localization	0	0.0
Genetic predisposition	0	0.0

BMI, Body mass index.

the absolute prerequisite for the comparative analysis of wall strain and wall stress.

Four-dimensional ultrasound with averaged models. 4D-US examination was performed using a commercial real-time 3D-echocardiography system (Artida, Toshiba Medical Systems) with a 3D transthoracic probe (Toshiba, PST-25SX, 1-4 MHz phased array matrix transducer) in a supine position after 5 minutes of rest. A starting point as a reference of each cardiac cycle was triggered by electrocardiogram at the end-diastole. In each case, a full volume dataset of 90° × 90° was registered from six electrocardiogram-triggered sub volumes of 90° × 15° recorded over six consecutive heart cycles and merged by embedded Toshiba software. The brachial arterial pressure was measured bilaterally by sphygmomanometry before and after the ultrasound examination. The arterial pressure at the time of 4D-US was later used as the patient-specific variable in finite element analysis. The diagnosis of AAA was established based on 2D-US imaging in a transverse cross-section and anterior-posterior plane using the leading edge to leading edge method.[19] For the comparison of the methods, a maximum systolic AAA diameter in 4D-US was additionally determined after adjusting the centerline with the same methodology as for 2D-US.

The 4D-US sequences were registered at a frequency of 4 MHz with a wavelength of the ultrasound signal at 0.39 mm, an opening angle between 55° and 110°, a frame rate of 26.3 ± 5.1 fps at a heart rate of 68 ± 12 bpm, and a resolution of 0.54 ± 0.10 mm/voxel. The length and width of the field of view, dependent mainly on the body mass index of the patients, were 11.1 ± 1.9 cm and 10.0 ± 2.1 cm, respectively, at a depth of 13.2 ± 2.4 cm.

Post-processing of the 4D-US data was conducted using the commercial Advanced Cardiac Package (ACP, Toshiba Medical Systems). The aneurysm wall in the end-diastolic configuration was manually segmented in the coronal and sagittal planes of the 4D-US image cross-section (A and B plane) five times (Fig 1). The speckle tracking algorithm provided by the commercial ACP utilized cubic template volumes of approximately 10 × 10 × 10 mm^3 for recognizing locally specific sonographic patterns. The motion of the centroid of these template volumes was described for each time step throughout the cardiac cycle by vectors of motion estimation points in Cartesian coordinates. The results of five speckle tracking runs were merged into one averaged model.[14,15] Averaging multiple segmentations involved combining the closest points of each segmentation into one point. Because the commercial software was designed for the left cardiac ventricle, the artificial pseudo-apex was removed from the initial model at the inflection point. This ensured that the 4D models of all 22 patients comprised only the aneurysm sac.[7] The resulting length of the final 4D models of the AAA sac was 50.8 ± 8.9 mm with 720 ± 61 motion estimation points. The Biot's in-plane strain tensor was calculated in local coordinates, using end-diastole as the reference configuration, with an in-house developed MATLAB (Edition 2022b, The MathWorks, Inc) toolbox. The results were verified using the commercial finite element solver Abaqus (Edition 6.12, Simulia — Dassault Systèmes). In-

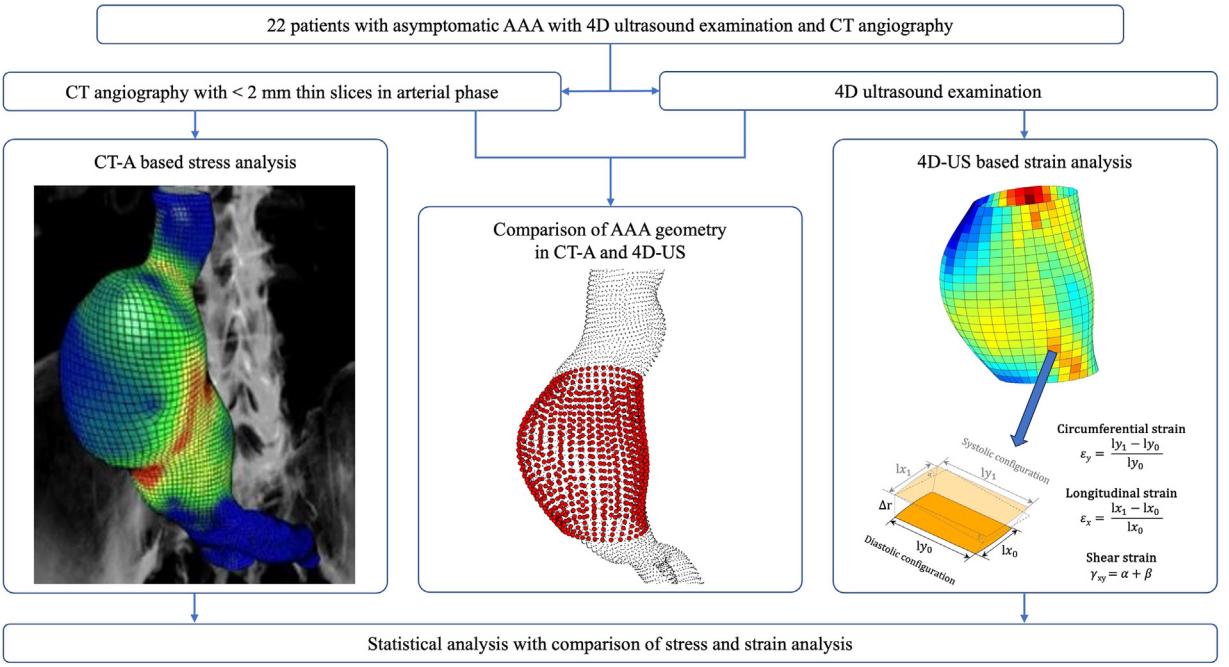

Fig 1. Statistical analysis with comparison of stress and strain analysis. *AAA*, Abdominal aortic aneurysm; *CT*, computed tomography; *CT-A*, computed tomography angiography; *4D*, four-dimensional; *3D*, three-dimensional; *US*, ultrasound.

plane components of the strain tensor were determined for each configuration in local element coordinate systems, considering the longitudinal, circumferential, and shear directions of the AAA.

Comparison of abdominal aortic aneurysm geometry in computed tomography angiography and 4-dimensional ultrasound. To ensure comparability between CTA and 4D-US derived models, the conformity of aneurysm geometry in 4D-US and CTA was verified. The CTAs were performed in a median of 7 days (min-max, 0-259 days) around the date of the 4D-US. The AAA wall in the CTA was reconstructed using the Vascular Modeling Tool Kit (VMTK, version 1.4.0, www.vmtk.org) through manual segmentation with the Colliding Fronts method. The resulting geometry, comprising approximately 60,000 points, was converted into a surface using the Marching Cubes algorithm and smoothed using the Taubin algorithm. As these geometries originate from different imaging modalities, it is essential to register the blood vessel geometries for an adequate comparison. For this reason, rigid body registration is employed to preserve the shape. During this algorithmic process, the goal is to align a moving point cloud (US) as closely as possible with a static point cloud (CTA). The algorithm iteratively follows these four steps to determine the required transformation and translation: (1) identification of the closest points between the two-point clouds; (2) calculation of the sum of the squared distances for these point pairs; (3) determination of the transformation and translation needed for optimal alignment; and (4) application of the determined transformation and translation. The resulting agreement of the 4D-US- and CTA-based geometries was quantified by mean point-to-point distance (MPPD). The MPPD is calculated as the average distance between all corresponding points in the two-point clouds, considering their coordinates in three-dimensional space (sum of all absolute Euclidean distance values divided by number of point pairs). The AAA geometry from 4D-US with the smallest MPPD was used for further evaluations.

Four-dimensional ultrasound-derived strain analysis. The deformation of the AAA wall in 4D-US is quantitatively characterized by strain analysis, determining longitudinal, circumferential, and shear strain (Fig 1). Strain amplitude is quantified by primary measured values such as mean and peak wall strain, as well as by secondary calculated parameters describing heterogeneity (spatial heterogeneity index and local strain ratio) (Table III). One strain value for each element characterizes the entire cardiac cycle and is calculated from strain peak-to-peak amplitudes, representing the difference between the largest and smallest local strain occurring for each element.

Computed tomography angiography-based finite element analysis stress analysis. FEA for assessing AAA wall stress was conducted on CTA with a thickness less than 2 mm in the arterial phase. The analysis utilized a

Table III. Glossary[7]

Parameter	Explanation
4D-US strain-derived parameters	
Wall strain	Change in distance between two points on the wall from the diastolic to systolic configuration as a measure of deformation
Circumferential and longitudinal strain	Relative change in length of the examined element in the circumferential direction and longitudinal axis of the vessel, respectively
Shear strain	Refers to the deformation characterized by a change in angles between initially perpendicular lines within an element
Primary variables	
Strain amplitude	Absolute difference between the maximum and minimum wall strain values
Mean strain amplitude	Average strain amplitude of all registered fields of the 3D model in the frame with the maximum strain amplitude
Local peak strain amplitude (later called peak strain)	Maximum strain amplitude of all registered fields of the 3D model in the frame with the maximum strain amplitude
Secondary variables	
Spatial heterogeneity index	Coefficient of variation of wall strain: ratio of the maximum standard deviation of local wall strain amplitudes and the mean wall strain amplitude
Local strain ratio	Ratio of maximum local and mean wall strain amplitude
FEA stress-derived parameters	
Wall stress	Calculated parameter describing forces occurring during deformation
Wall strength	Ability to withstand tensile stresses without rupture
PWS	Maximal value of tensile stress [kPa] in a specific AAA segment based on patient specific and geometrical boundary conditions
PWRI	Proportion of peak wall stress and wall strength (index from 0.0 to 1.0). In theory, a rupture occurs if the wall stress exceeds the wall strength (PWRI = 1)
RRED	RRED translates the biomechanical profile into the maximum diameter of an 'average AAA' with the same risk of rupture and PWRI[20]

AAA, Abdominal aortic aneurysm; *FEA*, finite element analysis; 4D-US, four-dimensional ultrasound; *PWRI*, Peak wall rupture risk index; *PWS*, peak wall stress; *RRED*, rupture risk equivalent diameter; *3D*, three-dimensional.

commercially available CE-certified semiautomated analysis software (A4clinic; VASCOPS GmbH) (Fig 1). The assessment of AAA wall stress involved three subsequent steps: (1) reconstruction of a 3D AAA geometry from CTA DICOM (Digital Imaging and Communication in Medicine) data; (2) mesh generation; and (3) calculation of biomechanical parameters, following the reported methodology.[21] The reconstruction of AAA anatomy respects both the outer AAA wall boundary and intraluminal thrombus volume (ILT) for voxel segmentation. FEA was conducted for the infrarenal aortic segment between the renal arteries and aortic bifurcation, calculating morphological (diameter/volume measurements) and biomechanical (PWS, PWRI, RRED) parameters related to homogeneous AAA wall properties. Patient-specific boundary conditions, including hypertension, AAA shape, smoking, gender, and ILT volume, were considered (Table II). The AAA models were fixed at the renal arteries and the aortic bifurcation, with no contact with surrounding organs. The AAA was pressurized by the mean arterial pressure, defined as one-third systolic pressure plus two-thirds diastolic pressure, onto the luminal layer. Blood pressure values from 4D-US strain analysis were retrospectively used for FEA computation. The aortic tissue was treated as an isotropic material model, assuming population averaged material parameters. The strength of the aneurysm wall is heterogeneous, and the applied FE models consider a wall strength model that accounts for local wall weakening influenced by intraluminal thrombus, gender, family history, and the ratio between the local diameter and the normal infrarenal aortic diameter. A PWRI between 0.5 and 1.0 indicates an increased risk of rupture.[5]

STATISTICAL ANALYSIS

The statistical analysis was conducted using the R package 'stats', Version 4.1.0, in consultation with the Institute for Biostatistics and Mathematical Modelling at Goethe University Frankfurt. The distribution of all variables was examined by the Shapiro-Wilk test. A *P*-value of $< .05$ was considered statistically significant for all tests. The correlation of clinical data, anatomical parameters, wall stress, and wall motion indices was assessed using the Pearson test for normally distributed variables and the Spearman' rank correlation analysis for non-normally distributed data. The results of the correlation analysis were presented in the form of a cross-correlation matrix, including *P*-values and correlation coefficients (r for

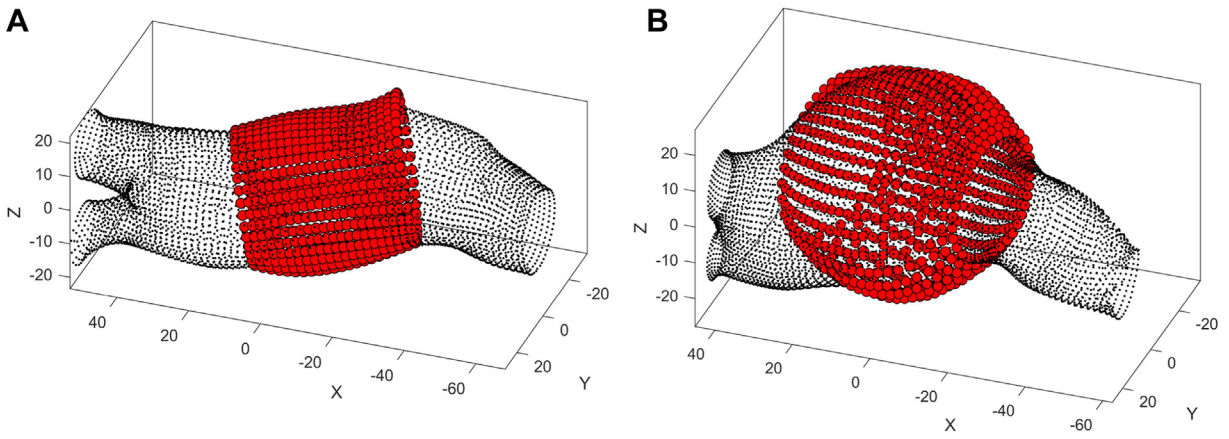

Fig 2. Example for abdominal aortic aneurysm (AAA) cases with the best (792 nodes with mean point-to-point distance [MPPD] of 1.21 mm) **(A)** and the poorest (756 nodes with MPPD of 2.93 mm) **(B)** conformity of the AAA geometry in four-dimensional ultrasound (4D-US) and computed tomography angiography (CT-A).

Pearson and ρ for Spearman's rank correlation). A correlation coefficient over 0.8 corresponds to a strong correlation, 0.6 to 0.8 corresponds to a moderately strong correlation, and 0.3 to 0.6 corresponds to a fair correlation, according to the interpretation of Chan.[22] If a relevant correlation was demonstrated, the data were evaluated for suitability for a linear regression according to Gauss Markov's theorem. The distribution of the standardized residuals was proved graphically and with Shapiro-Wilk test. The data were examined for homoscedasticity by means of a studentized Breusch-Pagan test, whereby a heteroscedasticity was assumed at $P < .05$. The heteroscedasticity of the data was corrected by applying the robust standard error according to the HC3 method. The interclass correlation coefficient (ICC) was calculated in R software with the "psych" package by one-way random-effects model (ICC_1) and interpreted according to the criteria of Koo and Li and corresponds to excellent reliability by ICC >0.90, good reliability by ICC 0.75 to 0.90, moderate reliability by ICC 0.50 to 0.75, and poor reliability by ICC under 0.50.[23] The reproducibility of all methods for measurement of maximum diameter was examined by Bland Altman plots with limits of agreement by mean ± 1.96 standard deviations.

RESULTS

Conformity of aneurysm anatomy reconstruction in four-dimensional ultrasound and computed tomography angiography

The comparison of aneurysm geometry in 4D-US and CTA was carried out in two models with 792 nodes in median (min-max, 612-864 nodes). The AAA geometry from 4D-US showed the best agreement with the CTA-derived aneurysm geometry in the fifth frame of the entire cardiac cycle by frame rate 26.3 ± 5.1 fps (Fig 2). The mean point-to-point distance between adjacent points of the 4D-US and CTA-derived geometry was 1.8 ± 0.4 mm (95% confidence interval [CI], 1.6-1.9 mm). Sonographic measurements of maximum aneurysm diameter in 2D- and 4D-US (mean ± standard deviation [SD], 50.1 ± 7.7 mm vs 46.5 ± 8.2 mm; $P > .05$) (Table IV) in the same patients are comparable, with a mean difference of 3.6 ± 4.9 mm and a very strong correlation ($r = 0.81$; 95% CI, 0.60-0.90; $P < .01$). However, the maximum AAA diameter measured in 4D-US is smaller than in CTA (46.5 ± 8.2 mm vs 53.2 ± 7.2 mm; $P < .05$) with a mean difference of −6.7 ± 3.6 mm but continues to correlate very strongly ($r = 0.90$; 95% CI, 0.76-0.96; $P < .01$). The ICCs for all raters and all measurements for maximum AAA diameter in 2D, 4D ultrasound, and CTA indicate moderate to good reliability (ICC_1 0.69 with 95% CI, 0.49-0.84; $P < .001$). The comparison of all measurement modalities is additional summarized in Fig 3 with Bland Altman plots.

Multifactorial characterization of the abdominal aortic aneurysm

Each aneurysm was characterized by determining anatomical, biomechanical, and kinematic indices. The study group includes AAAs with a maximum diameter ranging from 42.8 to 71.8 mm and an ILT thickness ranging from 4.0 to 43.2 mm (Table IV). Most aneurysms express a low rupture risk, as described by a mean PWRI of 0.37 ± 0.12. Three patients showed PWRI >0.5, with the maximum value being 0.69, corresponding to RRED values of 59.4, 69.0, and 73.0 mm, respectively. The aneurysm wall in the study cohort was characterized by a low mean strain amplitude, with a median of 0.89% (min-max, 0.27-2.50) in the circumferential direction, 0.83% (min-max, 0.22-2.25) in the longitudinal direction, and 1.27% (min-max, 0.68-3.53) for in-plane shear.

Table IV. The morphological, stress, and strain indices of all abdominal aortic aneurysms (*AAAs*) (n = 22)

	Mean ± SD	95% CI	Median (min-max)	IQR
Anatomical parameters				
Maximum AAA diameter in 2D-US, mm	50.1 ± 7.7	46.6-53.5	50.6 (36.4-64.0)	43.2-55.0
Maximum AAA diameter in 4D-US, mm	46.5 ± 8.4	42.9-50.1	46.5 (37.0-68.0)	39.5-49.8
Normal infrarenal aortic diameter, mm	21.2 ± 1.6	20.5-22.0	21.0 (18.0-24.0)	21.0-22.0
Maximum exterior AAA diameter, mm	53.2 ± 7.2	50.0-56.4	51.9 (42.8-71.8)	48.4-56.4
Maximum luminal AAA diameter, mm	35.5 ± 7.3	32.3-38.8	34.4 (24.1-50.9)	31.5-38.5
Maximum ILT thickness, mm	20.1 ± 9.9	15.7-24.5	18.7 (4.0-43.2)	14.0-25.5
Total vessel volume, cm^3	143.1 ± 57.4	117.6-168.5	136.2 (60.6-275.1)	99.3-172.5
Total lumen volume, cm^3	57.4 ± 28.2	44.9-69.9	48.2 (18.8-149.1)	45.2-64.8
Total ILT volume, cm^3	74.8 ± 51.5	51.9-97.6	55.6 (24.3-197.0)	33.5-89.2
CTA-based wall stress indices				
PWS, kPa	182.7 ± 39.7	165.1-200.3	179.3 (116.4-275.8)	156.6-195.7
Peak rupture risk index	0.37 ± 0.12	0.32-0.43	0.36 (0.20-0.69)	0.31-0.40
Rupture risk equivalent diameter, m	45.1 ± 11.3	40.1-50.2	43.8 (27.7-73.0)	39.2-48.2
4D-US based wall strain indices				
Circumferential strain				
Mean circumferential strain, %	1.02 ± 0.63	0.74-1.30	0.89 (0.27-2.50)	0.57-1.11
Peak circumferential strain, %	8.08 ± 2.89	6.80-9.36	7.34 (3.70-13.88)	6.17-9.44
Circumferential strain ratio	9.74 ± 4.31	7.82-11.65	9.45 (3.10-21.94)	7.14-11.02
Circumferential heterogeneity index	2.91 ± 1.29	2.34-3.48	2.80 (1.01-5.51)	2.01-3.38
Longitudinal strain				
Mean longitudinal strain, %	0.91 ± 0.50	0.69-1.13	0.83 (0.22-2.25)	0.54-1.18
Peak longitudinal strain, %	8.11 ± 3.01	6.78-9.45	7.76 (2.42-14.60)	5.98-9.99
Longitudinal strain ratio	11.06 ± 6.57	8.15-13.97	8.82 (4.57-29.25)	5.53-16.04
Longitudinal heterogeneity index	2.98 ± 1.84	2.16-3.80	2.49 (1.19-9.32)	1.82-3.50
In-plane shear				
Mean in-plane shear, %	1.55 ± 0.84	1.18-1.92	1.27 (0.68-3.53)	0.84-2.05
Peak in-plane shear, %	12.13 ± 5.38	9.75-14.52	11.44 (4.16-24.87)	8.60-15.43
In-plane shear ratio	8.96 ± 4.42	7.00-10.92	8.09 (2.80-24.18)	6.75-10.22
In-plane shear heterogeneity index	2.47 ± 1.04	2.01-2.93	2.29 (0.91-6.08)	19.57-28.93

CI, Confidence interval; *CTA*, computed tomography angiography; *4D*, four-dimensional; *ILT*, intraluminal thrombus; *IQR*, interquartile range; *PWS*, peak wall stress = maximum vs mises stress in the AAA wall; *SD*, standard deviation; *2D*, two-dimensional; *US*, ultrasound.

Interaction of clinical, anatomical, biomechanical, and kinematic indices in abdominal aortic aneurysms

Clinical data and their impact on anatomical variables and stress/strain analysis. The clinical data include age, weight, height, and systolic and diastolic systemic blood pressure only. A normal infrarenal aortic diameter moderately correlates with patient age ($\rho = 0.64$; $P < .01$). The diameter of non-aneurysmal aorta by study cohort, measured at the level of renal arteries, is greater the older the patients are (0.16 mm per 1 year of life by adjusted $R^2 = 0.38$). Patient height shows a fair correlation with peak wall stress ($r = 0.51$; $P < .05$) and peak longitudinal strain ($r = -0.47$; $P < .05$). No influence of systolic blood pressure on wall stress and wall motion indices was found. Diastolic blood pressure showed a fair correlation with the mean ($\rho = 0.47$; $P < .05$) and peak circumferential strain ($r = 0.51$; $P < .05$), as well as with peak in-plane shear ($r = 0.46$; $P < .05$). However, the predictive value of the clinical data for stress and strain analysis is very low (adjusted R^2 value for all above parameters <0.25).

Interaction of anatomical parameters and wall stress analysis. The FEA and determination of PWS and PRRI involve multiple interactions with anatomical parameters from 4D-US (Fig 4). The PWS shows a fair correlation with the maximum AAA diameter in 2D-US ($r = 0.54$; $P < .01$) and 4D-US ($r = 0.53$; $P < .05$), a moderately strong correlation with the maximum exterior AAA diameter ($r = 0.63$; $P < .01$), and total vessel volume in CTA ($r = 0.72$; $P < .001$). Additionally, a strong correlation between PWS and the maximum luminal AAA diameter ($\rho = 0.92$; $P < .001$) and total lumen volume ($\rho = 0.80$; $P < .001$) is observed.

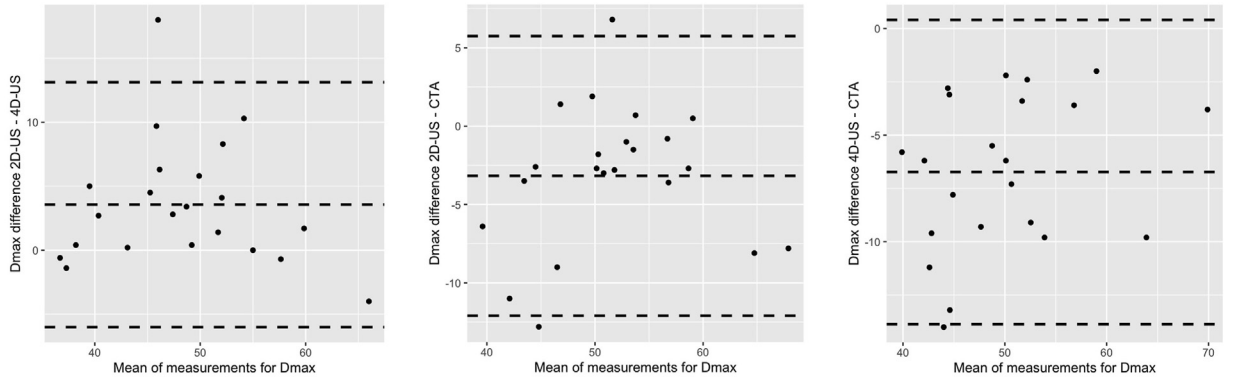

Fig 3. Bland Altman plots for measurements of maximum abdominal aortic aneurysm (AAA) diameter (DMax) in two-dimensional ultrasound (2D-US), four-dimensional ultrasound (4D-US), and computed tomography angiography (CTA).

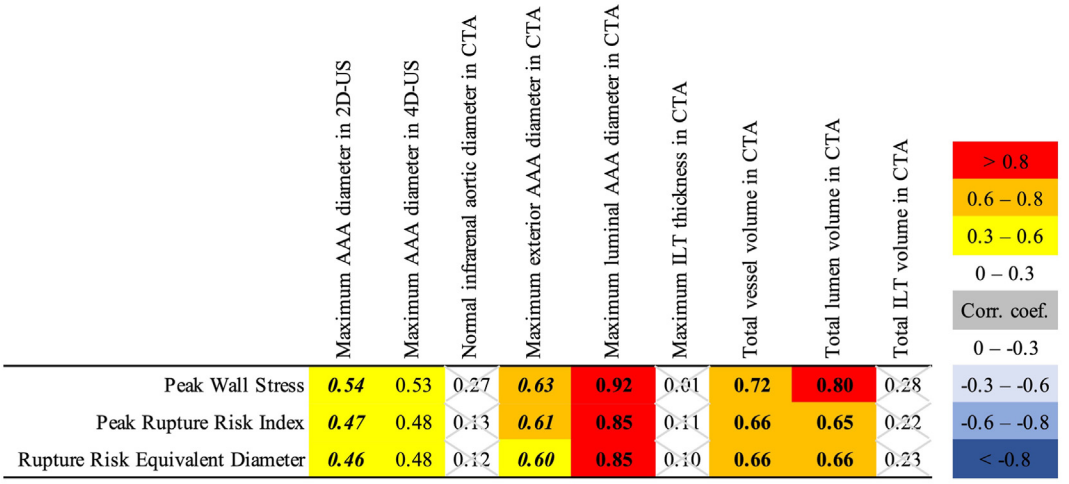

Fig 4. Cross-correlations of anatomical- vs wall stress-related parameters. The crossed boxes mark insignificant results. The normal, cursive bold, and bold fonts mark $P < .05$, $P < .01$, and $P < .001$, respectively. *AAA*, Abdominal aortic aneurysm; *CTA*, computed tomography angiography; *4D*, four-dimensional; *ILT*, intraluminal thrombus; *2D*, two-dimensional; *US*, ultrasound.

Assuming a linear regression model, a growth of the maximum AAA diameter in 2D-US, 4D-US, and CTA, of maximum luminal AAA diameter by 1 mm, or of total vessel volume, of total lumen volume by 1 cm^3, is associated with an increase of PWS by 2.77 kPa ($P < .01$; adjusted R^2 0.25), 2.57 ($P < .01$; adjusted R^2 0.25), 3.46 kPa ($P < .01$; adjusted R^2 0.36), 4.98 kPa ($P < .01$; adjusted R^2 0.83), 0.49 kPa ($P < .01$; adjusted R^2 0.49), and 1.13 kPa ($P < .01$; adjusted R^2 0.62), respectively.

The PPRI correlates strongly with the PWS ($\rho > 0.90$; $P < .001$) and is influenced by the above-mentioned anatomical parameters with equal strength accordingly. Both parameters PPRI and RRED provide the same statements ($\rho = 0.999$; $P < .001$), but in two formats. Isolated observation of the intraluminal thrombus does not provide any significant information in the determination of PWS.

Correlation of anatomical parameters with wall strain indices. The maximum AAA diameter in 2D-US shows a fair negative correlation with the mean circumferential, longitudinal, and in-plane shear strain ($\rho = -0.46$; $r = -0.45$; $\rho = -0.47$; $P < .05$ for all) (Fig 5). We found no significant correlation between the maximum AAA diameter in 4D-US and any strain indices. Mean longitudinal strain decreases with increasing normal infrarenal aortic diameter ($\rho = -0.56$; $P < .01$). The circumferential strain ratio as an indicator of wall motion heterogeneity increases with the normal and aneurysmal aortic diameter ($r = 0.47$ for maximum AAA diameter in 2D-US and $\rho = 0.43$ for normal infrarenal aortic diameter in CTA; $P < .05$ for both). However, all these parameters have weak statistical predictive value in the linear regression model (adjusted $R^2 < 0.30$). Statistically significant observations in the secondary wall motion

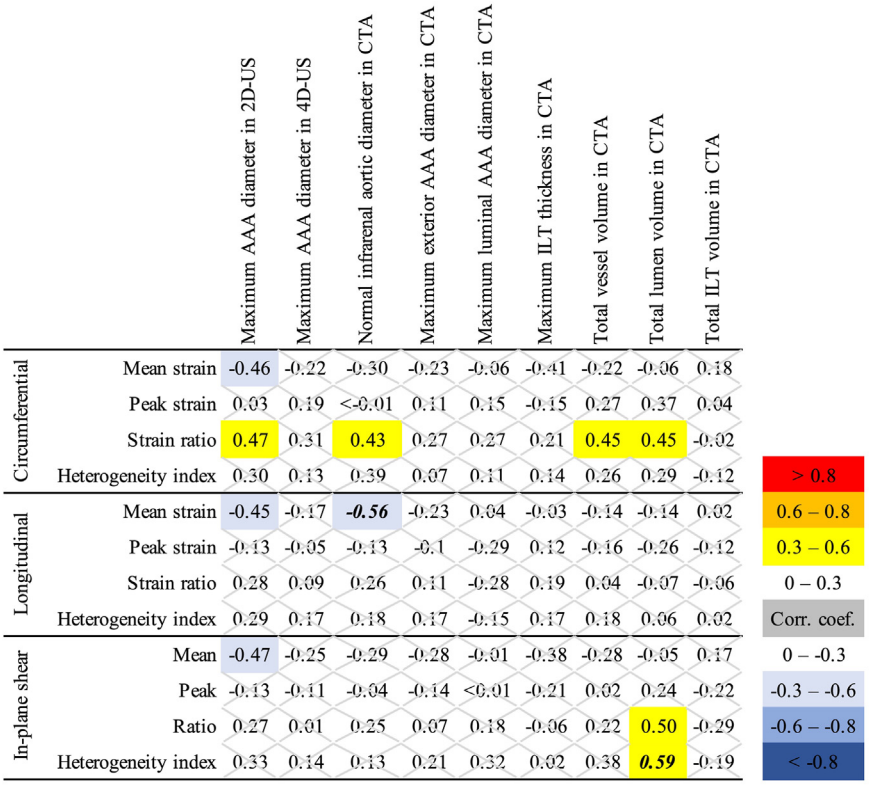

Fig 5. Cross-correlations of anatomical- vs wall strain-related parameters. The crossed boxes mark insignificant results. The normal, cursive bold, and bold fonts mark $P < .05$, $P < .01$, and $P < .001$, respectively. *AAA*, Abdominal aortic aneurysm; *CTA*, computed tomography angiography; *4D*, four-dimensional; *ILT*, intraluminal thrombus; *2D*, two-dimensional; *US*, ultrasound.

indices, such as strain ratio or heterogeneity index, should be interpreted as random effects if there are no changes in the primary indices like mean and peak strain.

Correlation of strain and stress analysis. The comparison of wall strain and wall stress indices shows no direct quantitative correlation (Fig 6).

DISCUSSION

Appropriate assessment of AAA rupture risk and timely aneurysm care, set as a goal, aims to reduce AAA- and surgery-related mortality. Although the maximum aneurysm diameter is still used as the primary prognostic criterion for AAA rupture risk, early attempts have been made to bridge the gap between aneurysm morphology and wall stress.[24,25] Dynamic ultrasound studies from the early 2000s suggest a potential link between strain analyses and the risk of AAA rupture.[26] Our study, for the first time, compares strain- and stress-derived global parameters in the characterization of AAAs. A challenge in the current evaluation is the comparison of two biomechanical methods based on strain and stress analysis from two different imaging methods (CTA and 4D-US). We compare a static aortic geometry based on CTA with a dynamic imaging in 4D-US, where each method has its own advantages and disadvantages with different approaches to biomechanical aspects. The CTA-based FEA model calculates the resulting wall stress from total wall strain, whereas the wall strain of the 4D-US refers to the cyclic strain. The CTA provides the highest resolution for imaging anatomical structures, whereas the 4D-US focuses on identification of the dynamic properties of the aorta with a reduced spatial resolution for the aortic anatomy depending on the phase of the cardiac cycle, which is the cause of a significant deviation in the determination of the maximum aneurysm diameter in the CTA and 4D-US by already known unavoidable observer-related uncertainty in the determination of the maximum AAA diameter in the CTA and 2D-US.[27] Nevertheless, the present analysis and methodology confirm the good agreement of the complex three-dimensional AAA geometry from 4D-US and CTA.

The comparison of the interaction between wall strain and wall stress in AAA remains a challenging task in biomechanics, as the imaging requirements for both analyses differ. The high spatial resolution of CTA, a significant advantage for imaging aneurysm geometry, is utilized for determining wall stress. However, conclusions drawn from previous experience do not allow a clear discretization of ruptured and unruptured aneurysms

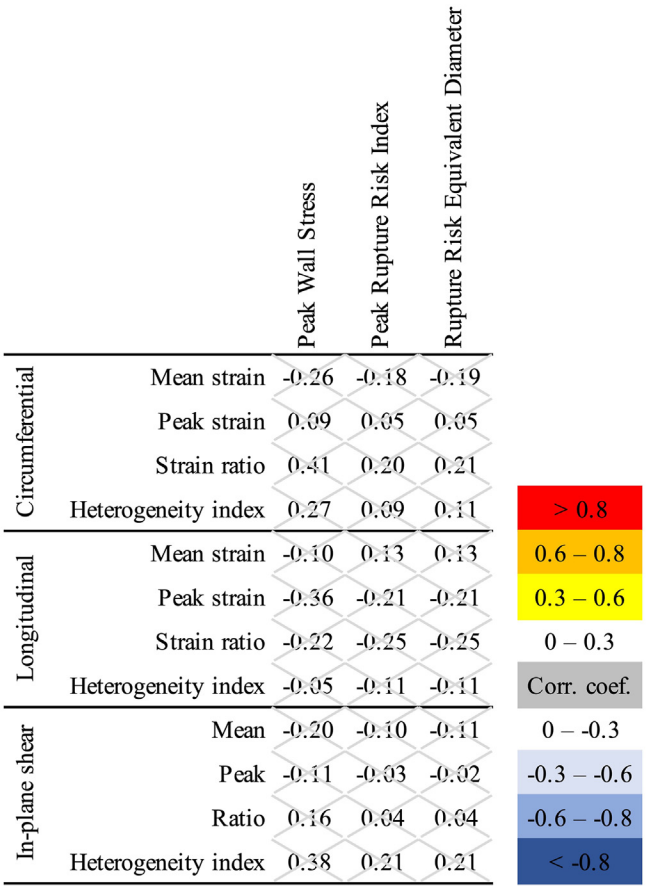

Fig 6. Cross-correlations of wall strain- vs wall stress-related parameters. The crossed boxes mark insignificant results. The normal, cursive bold, and bold fonts mark $P < .05$, $P < .01$, and $P < .001$, respectively.

based on single stress analysis, as FEA does not a priori differentiate between intact and ruptured AAAs with sufficient specificity and sensitivity as a diagnostic test.[5] The main limitation of CTA, in addition to the usual disadvantages such as radiation and contrast medium exposure, is the imaging of the static AAA geometry. Van Disseldorp et al were able, for the first time, to bridge the gap between a dynamic representation from 4D-US and the static visualization of the aneurysm in CTA, demonstrating high agreement for wall stress indices.[28]

The strain analysis, on the other hand, requires information from dynamic imaging modalities with high spatial and temporal resolution of the systolic and diastolic configuration, such as magnetic resonance angiography and 3D- or 4D-US. These modalities are associated with considerable resources in clinical routine and are therefore limited to intact aneurysms. Due to the lack of dynamic imaging before and after rupture, it is challenging to establish a connection between strain analysis and an aneurysm rupture risk. Therefore, previous publications focus on describing the dynamic properties of the aortic aneurysm with the identification of suspected strain patterns.[7,9,10,29] However, strain analysis provides additional information about the patient-specific material properties of the aneurysm wall.[12] The present study shows a decrease in mean circumferential, longitudinal, and shear strain the larger the aneurysms are, indicating progressive stiffening of the aneurysm wall. The decreased compliance in the aneurysmal aortic walls is considered an important contribution in rupture mechanisms. From this perspective, stress and strain analysis describe different processes in the aneurysm wall, which could complement each other in creating the individual risk profile.

The aortic wall stress shows a strong correlation with the maximum exterior as well as luminal AAA diameter in our evaluation, confirming previous scientific reports.[20] The AAA geometry and systemic blood pressure are so dominant in the calculation of wall stress that Joldes et al postulate that there is no need to specify further parameters such as material properties, boundary conditions, and patient characteristics.[30] However, Polzer et al were able to demonstrate that a complete biomechanical rupture risk assessment has significantly better predictive power, even 9 months in advance, than the maximum diameter itself.[31] Although we do not find any direct correlation between the stress- and strain-derived indices in the current comparison, both methods might have complementary effects. The complementary statements include information on the local deformation of the aneurysm wall with determination of the mean/peak strain and heterogeneity describing parameters, as well as on local differences in distensibility and stiffness. Stress analysis, on the other hand, can firstly be optimized by information from the 4D-US about the individual material properties and, secondly, can provide more details about the local stress distribution. FEA assumes homogeneous wall thickness and material properties. If, for example, large strains are observed in an area, that are described in finite element model to have average stress values at the same time, the model assumptions for prediction of aneurysm rupture based on stress analysis will not be fulfilled, because wall thickness or stiffness might be drastically reduced in this region. Literature findings indicate that rupture occurs in regions with locally reduced wall thickness. Reduced stiffness and increased compliance might indicate, respectively, a weakening of the wall or less degenerated wall properties. Thus, the combination of both approaches allows identification of conspicuous wall regions that might be prone to rupture. Because the mechanism of an aneurysm rupture is not clear and the prediction models do not allow for unambiguous statements, the multifactorial analysis may be able to provide more conclusions about the rupture prediction.

However, the role of the intraluminal thrombus is discussed controversially. The thrombus thickness showed no direct correlation with the stress and strain-derived indices. We only observe a positive correlation of the peak wall stress with the increasing maximum luminal AAA diameter. Lorandon et al even claim that stress analysis is not capable of rupture prediction in aneurysms with intraluminal thrombus.[32] The previous considerations based on a single study will be further developed based on follow-up observations. Zschäpitz et al emphasize not only the role of changing AAA geometry but also the influence of morphological thrombus on the transformation of regions with high wall stress.[33] For this reason, the complementary effect of the morphologica and, stress- and strain-derived indices with the use of artificial intelligence algorithms might support the prospective evaluation of AAA rupture risk in the future perspective.[34]

The current statistical analysis has an absolutely exploratory character. The individual, potentially relevant parameters must be proved in the future by validation study with a larger number of patients and examination of discretization power by a higher significance level with corresponding correction in multifactorial analysis for single indices.

LIMITATIONS

The current analysis is based on a small cohort with inhomogeneous aneurysm size. The aneurysms are characterized by a slightly to moderately increased risk of rupture according to PWRI calculations. For both calculations, homogeneous blood pressure values were used that do not reflect long-term blood pressure values of the individual patients. Aneurysm imaging with A4-Clinics covers a region from the renal arteries to the aortic bifurcation. The strain analysis refers to a defined area of the AAA sac.

CONCLUSION

The study presents an algorithm for AAA 3D reconstruction derived from CTA and 4D-US to compare static and dynamic calculations in AAAs. The strain-related parameters show no direct correlation with wall stress describing indices. However, the stress and strain analyses might provide important complementary information on the biomechanical and kinematic properties of the aneurysmal wall for patient-specific AAA rupture risk estimation.

AUTHOR CONTRIBUTIONS

Conception and design: WD, CB, AW, PE
Analysis and interpretation: WD, MS, PE
Data collection: WD
Writing the article: WD, MS, PE
Critical revision of the article: CB, AW, KO, DB
Final approval of the article: WD, MS, CB, AW, KO, DB, PE
Statistical analysis: WD, MS
Obtained funding: WD, CB, AW, DB, PE
Overall responsibility: WD

FUNDING

This work was funded by the Adolf Messer Foundation and the Ministry of Higher Education, Research, and the Arts (HMWK, Hesse, Germany). No institutions have any involvement in the study design, collection, analysis, interpretation of data, by writing and publication of the manuscript.

DISCLOSURES

None.

REFERENCES

1. Fillinger MF, Marra SP, Raghavan ML, Kennedy FE. Prediction of rupture risk in abdominal aortic aneurysm during observation: wall stress versus diameter. *J Vasc Surg*. 2003;37:724–732.
2. Farotto D, Segers P, Meuris B, Vander Sloten J, Famaey N. The role of biomechanics in aortic aneurysm management: requirements, open problems and future prospects. *J Mech Behav Biomed Mater*. 2018;77:295–307.
3. Romo A, Badel P, Duprey A, Favre JP, Avril S. In vitro analysis of localized aneurysm rupture. *J Biomech*. 2014;47:607–616.
4. Erhart P, Hyhlik-Dürr A, Geisbüsch P, et al. Finite element analysis in asymptomatic, symptomatic, and ruptured abdominal aortic aneurysms: in search of new rupture risk predictors. *Eur J Vasc Endovasc Surg*. 2015;49:239–245.
5. Erhart P, Roy J, de Vries JPPM, et al. Prediction of rupture sites in abdominal aortic aneurysms after finite element analysis. *J Endovasc Ther*. 2016;23:115–120.
6. van Disseldorp EMJ, Petterson NJ, Rutten MCM, van de Vosse FN, van Sambeek MRHM, Lopata RGP. Patient specific wall stress analysis and mechanical characterization of abdominal aortic aneurysms using 4D ultrasound. *Eur J Vasc Endovasc Surg*. 2016;52:635–642.
7. Derwich W, Wittek A, Hegner A, Fritzen CP, Blase C, Schmitz-Rixen T. Comparison of abdominal aortic aneurysm sac and neck wall motion with 4D ultrasound imaging. *Eur J Vasc Endovasc Surg*. 2020;60:539–547.
8. van Disseldorp E, van den Hoven M, van de Vosse F, van Sambeek M, Lopata R. Reproducibility assessment of ultrasound-based aortic stiffness quantification and verification using Bi-axial tensile testing. *J Mech Behav Biomed Mater*. 2020;103:103571.
9. Derwich W, Wittek A, Pfister K, et al. High resolution strain analysis comparing aorta and abdominal aortic aneurysm with real time three dimensional speckle tracking ultrasound. *Eur J Vasc Endovasc Surg*. 2016;51:187–193.
10. Derwich W, Keller T, Filmann N, et al. Changes in aortic diameter and wall strain in progressing abdominal aortic aneurysms. *J Ultrasound Med*. 2023;42:1737–1746.
11. Wittek A, Derwich W, Karatolios K, et al. A finite element updating approach for identification of the anisotropic hyperelastic properties of normal and diseased aortic walls from 4D ultrasound strain imaging. *J Mech Behav Biomed Mater*. 2016;58:122–138.
12. Wittek A, Derwich W, Fritzen CPCP, Schmitz-Rixen T, Blase C. Towards non-invasive in vivo characterization of the pathophysiological state and mechanical wall strength of the individual human AAA wall based on 4D ultrasound measurements. *Z Angew Math Mech*. 2018;98:2275–2294.
13. Wittek A, Karatolios K, Bihari P, et al. In vivo determination of elastic properties of the human aorta based on 4D ultrasound data. *J Mech Behav Biomed Mater*. 2013;27:167–183.
14. Wittek A. *Mechanical and Pathophysiological in Vivo Characterization of the Individual Aortic Wall Based on 4D Ultrasound Imaging*. Siegen: University Siegen; 2022. Available at:. Accessed April 1, 2024. http://dx.doi.org/10.25819/ubsi/10045.
15. Hegner A, Wittek A, Derwich W, Huß A, Gámez AJ, Blase C. Using averaged models from 4D ultrasound strain imaging allows to significantly differentiate local wall strains in calcified regions of

abdominal aortic aneurysms. *Biomech Model Mechanobiol*. 2023;22:1709–1727.
16. Derwich W, Wiedemann A, Wittek A, Filmann N, Blase C, Schmitz-Rixen T. Intra- and interobserver variability of 4D ultrasound examination of the infrarenal aorta. *J Ultrasound Med*. 2021;40:2391–2402.
17. Cho IJ, Lee J, Park J, et al. Feasibility and accuracy of a novel automated three-dimensional ultrasonographic analysis system for abdominal aortic aneurysm: comparison with two-dimensional ultrasonography and computed tomography. *Cardiovasc Ultrasound*. 2020;18:24.
18. Teutelink A, Cancrinus E, Van De Heuvel D, Moll F, De Vries JP. Preliminary intraobserver and interobserver variability in wall stress and rupture risk assessment of abdominal aortic aneurysms using a semiautomatic finite element model. *J Vasc Surg*. 2012;55:326–330.
19. Wanhainen A, Verzini F, Van Herzeele I, et al. European society for vascular surgery (ESVS) 2019 clinical practice guidelines on the management of abdominal aorto-iliac artery aneurysms. *Eur J Vasc Endovasc Surg*. 2019;57:8–93.
20. Gasser TC, Nchimi A, Swedenborg J, et al. A novel strategy to translate the biomechanical rupture risk of abdominal aortic aneurysms to their equivalent diameter risk: method and retrospective validation. *Eur J Vasc Endovasc Surg*. 2014;47:288–295.
21. Auer M, Gasser TC. Reconstruction and finite element mesh generation of abdominal aortic aneurysms from computerized tomography angiography data with minimal user interactions. *IEEE Trans Med Imaging*. 2010;29:1022–1028.
22. Chan YH. Biostatistics: correlational analysis. *Singapore Med J*. 2003;44:614–619.
23. Koo TK, Li MY. A guideline of selecting and reporting intraclass correlation coefficients for reliability research. *J Chiropr Med*. 2016;15:155–163.
24. Elger DF, Blackketter DM, Budwig RS, Johansen KH. The influence of shape on the stresses in model abdominal aortic aneurysms. *J Biomech Eng*. 1996;118:326–332.
25. Vorp DA, Raghavan ML, Webster MW. Mechanical wall stress in abdominal aortic aneurysm: influence of diameter and asymmetry. *J Vasc Surg*. 1998;27:632–639.
26. Wilson KA, Lee AJ, Hoskins PR, Fowkes FGR, Ruckley CV, Bradbury AW. The relationship between aortic wall distensibility and rupture of infrarenal abdominal aortic aneurysm. *J Vasc Surg*. 2003;37:112–117.
27. Bredahl K, Sandholt B, Lönn L, et al. Three-dimensional ultrasound evaluation of small asymptomatic abdominal aortic aneurysms. *Eur J Vasc Endovasc Surg*. 2015;49:289–296.
28. Van Disseldorp E, Petterson N, Rutten M, Van De Vosse F, van Sambeek M, Lopata R. Patient specific wall stress analysis and mechanical characterization of abdominal aortic aneurysms using {4D} ultrasound. *Eur J Vasc Endovasc Surg*. 2016;52:635–642.
29. Wittek A, Blase C, Derwich W, Schmitz-Rixen T, Fritzen CPCP. Characterization of the mechanical behavior and pathophysiological state of abdominal aortic aneurysms based on 4D ultrasound strain imaging. In: Ferraro P, Grilli S, Ritsch-Marte M, Hitzenberger CK, eds. *Optical Methods for Inspection, Characterization, and Imaging of Biomaterials III*. Vol 10333. 2017:1033303.
30. Joldes GR, Miller K, Wittek A, Doyle B. A simple, effective and clinically applicable method to compute abdominal aortic aneurysm wall stress. *J Mech Behav Biomed Mater*. 2016;58:139–148.
31. Polzer S, Gasser TC, Vlachovský R, et al. Biomechanical indices are more sensitive than diameter in predicting rupture of asymptomatic abdominal aortic aneurysms. *J Vasc Surg*. 2020;71:617–626.
32. Lorandon F, Rinckenbach S, Settembre N, Steinmetz E, Mont LS Du, Avril S. Stress analysis in AAA does not predict rupture location correctly in patients with intraluminal thrombus. *Ann Vasc Surg*. 2022;79:279–289.
33. Zschäpitz D, Bohmann B, Lutz B, et al. Rupture risk parameters upon biomechanical analysis independently change from vessel geometry during abdominal aortic aneurysm growth. *JVS Vasc Sci*. 2022;4:100093.
34. Forneris A, Beddoes R, Benovoy M, Faris P, Moore RD, Di Martino ES. AI-powered assessment of biomarkers for growth prediction of abdominal aortic aneurysms. *JVS Vasc Sci*. 2023;4:100119.

Submitted Dec 12, 2023; accepted Mar 9, 2024.